Trapped Fermions with Density Imbalance in the Bose-Einstein Condensate Limit

P. Pieri and G. C. Strinati
Dipartimento di Fisica, Università di Camerino, I-62032 Camerino, Italy
(Received 14 December 2005; published 21 April 2006)

We analyze the effects of imbalancing the populations of two-component trapped fermions, in the Bose-Einstein condensate limit of the attractive interaction between different fermions. Starting from the gap equation with two fermionic chemical potentials, we derive a set of coupled equations that describe composite bosons and excess fermions. We include in these equations the processes leading to the correct dimer-dimer and dimer-fermion scattering lengths. The coupled equations are then solved in the Thomas-Fermi approximation to obtain the density profiles for composite bosons and excess fermions, which are relevant to the recent experiments with trapped fermionic atoms.

DOI: 10.1103/PhysRevLett.96.150404 PACS numbers: 03.75.Hh, 03.75.Ss

Two recent experimental studies of superfluid trapped Fermi atoms with imbalanced populations [1,2] have raised novel interest in the physics of the BCS-Bose-Einstein condensation (BEC) crossover. Density profiles of the two fermionic species [1,2] as well as vortices [1] have been detected. A quantum phase transition to the normal state on the weak-coupling side of the BCS-BEC crossover [1] as well as a phase separation in the crossover region [1,2], both driven by density imbalance, have been identified.

The many-body problem becomes richer when the fermionic populations are imbalanced, since this additional degree of freedom gives rise to new phenomena. The effects of density imbalance on fermionic superfluids have been studied theoretically mostly within mean field and on the weak-coupling (BCS) side of the crossover, both for the homogeneous [3] and trapped case [4]. Only recently these calculations have been extended to cover the BCS-BEC crossover [5,6], but without considering the effects of the trap which are essential to account for the experimental results with density imbalance [1,2].

The effects of the trap are especially important to produce a phase separation between the density profiles of the two fermionic species, which may otherwise remain at the verge of an instability for a homogeneous system. In this respect, consideration of the strong-coupling (BEC) side of the crossover appears relevant, since phase separation is more robust in this limit. (On the weak-coupling side, on the other hand, density imbalance acts to quickly destroy the superfluid phase.) In addition, on the BEC side theoretical studies can rely on more accurate treatments beyond mean field, by exploiting the diluteness condition of the system. From previous experience on the BCS-BEC crossover, one expects the results obtained on the BEC side to be qualitatively similar to those occurring near unitarity.

Accordingly, in this Letter we analyze the BEC side of the crossover where trapped fermions with imbalanced populations get rearranged into a system of composite bosons (dimers) plus a number of excess (unpaired) fermions. We consider specifically the limit of low temperature, whereby all dimers are condensed, and derive a set of coupled equations describing the dimers and the excess fermions, which are interacting through dimer-dimer and dimer-fermion scattering processes. To the extent that the system is dilute, we can consider these processes exhaustively. Because of these interactions, the mutual effects between dimers and excess fermions need to be dealt with self-consistently in the equations. This results in a nontrivial evolution of their density profiles as the degree of density imbalance increases. We determine numerically these density profiles within a local approximation and find that dimers and excess fermions tend to reside in different spatial regions of the trap. We also show how from these profiles one can extract the dimer-fermion scattering length.

We consider first the derivation of the above coupled equations within mean field. When the populations of the two fermionic species (labeled by $\uparrow$ and $\downarrow$) are equal, it has already been shown [7] that the Bogoliubov-de Gennes (BdG) equations for trapped fermions can be mapped in the BEC limit onto the Gross-Pitaevskii equation for composite bosons, the only remnant of the original fermionic nature residing in the dimer-dimer scattering length entering that equation. In the case of interest here of imbalanced populations, this mapping has to be reconsidered since composite bosons and excess fermions coexist and mutually interact.

The presence of two fermionic species with populations $N_\uparrow$ and $N_\downarrow$ requires us to introduce two chemical potentials $\mu_\uparrow$ and $\mu_\downarrow$. (For definiteness, we assume $N_\uparrow \geq N_\downarrow$.) In analogy to Ref. [7], we consider the noninteracting Green's functions which satisfy the equation $[i\omega_s - \mathcal{H}_\sigma(\mathbf{r})]\tilde{\mathcal{G}}_0(\mathbf{r}, \mathbf{r}'; \omega_s|\mu_\sigma) = \delta(\mathbf{r} - \mathbf{r}')$, being subject to the trap potential $V(\mathbf{r})$ entering the single-particle Hamiltonian $\mathcal{H}_\sigma(\mathbf{r}) = -\nabla^2/(2m) + V(\mathbf{r}) - \mu_\sigma$. Here, $\sigma = (\uparrow, \downarrow)$, m is the fermion mass, and $\omega_s = (2s+1)\pi/\beta$ (s integer) is a fermionic Matsubara frequency (β being the inverse temperature). With these noninteracting Green's functions we form the matrix:

$$\hat{\mathcal{G}}_0(\mathbf{r}, \mathbf{r}'; \omega_s) = \begin{bmatrix} \tilde{\mathcal{G}}_0(\mathbf{r}, \mathbf{r}'; \omega_s|\mu_\uparrow) & 0 \\ 0 & -\tilde{\mathcal{G}}_0(\mathbf{r}', \mathbf{r}; -\omega_s|\mu_\downarrow \end{bmatrix}.$$

The corresponding interacting single-particle Green's functions within mean field are obtained by solving the integral equation:

$$\hat{\mathcal{G}}(\mathbf{r},\mathbf{r}';\omega_s) = \hat{\mathcal{G}}_0(\mathbf{r},\mathbf{r}';\omega_s) + \int d\mathbf{r}'' \hat{\mathcal{G}}_0(\mathbf{r},\mathbf{r}'';\omega_s)\hat{\mathrm{B}}(\mathbf{r}'')\hat{\mathcal{G}}(\mathbf{r}'',\mathbf{r}';\omega_s), \quad (1)$$

where

$$\hat{\mathrm{B}}(\mathbf{r}) = \begin{bmatrix} 0 & \Delta(\mathbf{r}) \\ \Delta^*(\mathbf{r}) & 0 \end{bmatrix}$$

contains the local gap $\Delta(\mathbf{r})$. Solution of the integral Eq. (1) is equivalent to the solution of the BdG equations in the trap in the presence of density imbalance.

The elements G_{11} and G_{22} of the matrix (1) determine the local densities, while the element G_{21} determines the local gap. To obtain the coupled equations of interest we expand them up to order Δ^2 and Δ^3, respectively, in analogy to what was done in Ref. [7] in the absence of density imbalance. The gap equation reads:

$$\begin{aligned} 0 &= \frac{1}{v_0}\Delta^*(\mathbf{r}) - \frac{1}{\beta}\sum_s e^{-i\omega_s\eta}G_{21}(\mathbf{r},\mathbf{r};\omega_s) \\ &\cong \frac{1}{2}b_0(\mathbf{r})\nabla^2\Delta^*(\mathbf{r}) + \left[\frac{1}{v_0} + a_0(\mathbf{r})\right]\Delta^*(\mathbf{r}) \\ &\quad + c_0(\mathbf{r})|\Delta(\mathbf{r})|^2\Delta^*(\mathbf{r}), \end{aligned} \quad (2)$$

where η is a positive infinitesimal and $v_0(<0)$ is the strength of the attractive contact potential between fermions of opposite spins. As in Ref. [7], the coefficients a_0, b_0, and c_0 of Eq. (2) are expressed in terms of the Green's functions $\tilde{\mathcal{G}}_0(\mu_\sigma)$, here with chemical potentials μ_σ appropriate to imbalanced populations. While $b_0(\mathbf{r}) \cong ma_{\mathrm{F}}/(16\pi)$ retains the same value as for equal populations (where a_{F} is the fermionic scattering length), a_0 and c_0 are affected by density imbalance in a relevant way. With the local *ansatz* for $\tilde{\mathcal{G}}_0(\mu_\sigma)$ introduced in Ref. [7] in terms of the Green's functions of the associated homogeneous problem, we obtain at low temperature:

$$\frac{1}{v_0} + a_0(\mathbf{r}) = \frac{1}{v_0} + \int \frac{d\mathbf{k}}{(2\pi)^3}\frac{\{1 - f[\frac{\mathbf{k}^2}{2m} + V(\mathbf{r}) - \mu_\uparrow] - f[\frac{\mathbf{k}^2}{2m} + V(\mathbf{r}) - \mu_\downarrow]\}}{\frac{\mathbf{k}^2}{m} - \mu_\uparrow - \mu_\downarrow + 2V(\mathbf{r})} \cong \frac{m^2 a_{\mathrm{F}}}{8\pi}[\mu_{\mathrm{B}} - 2V(\mathbf{r})] - \frac{1}{\epsilon_0}\delta n_f(\mathbf{r}), \quad (3)$$

where $f(\epsilon) = [\exp(\beta\epsilon) + 1]^{-1}$ is the Fermi function. We have made use of the fermion bound-state equation with binding energy $\epsilon_0 = (ma_{\mathrm{F}}^2)^{-1}$, introduced the bosonic chemical potential $\mu_{\mathrm{B}} = \mu_\uparrow + \mu_\downarrow + \epsilon_0$, and anticipated that $\mu_\downarrow \sim -\epsilon_0$ while $\mu_\uparrow \sim \epsilon_{\mathrm{F}}(\delta n)$, where $\epsilon_{\mathrm{F}}(\delta n)$ is the Fermi level of *free* excess fermions with density:

$$\delta n_f(\mathbf{r}) = \int \frac{d\mathbf{k}}{(2\pi)^3} f\left[\frac{\mathbf{k}^2}{2m} + V(\mathbf{r}) - \mu_\uparrow\right]. \quad (4)$$

Equation (3) can be cast in the meaningful form

$$\frac{1}{v_0} + a_0(\mathbf{r}) \cong \frac{m^2 a_{\mathrm{F}}}{8\pi}\left[\mu_{\mathrm{B}} - 2V(\mathbf{r}) - \frac{3\pi a_{\mathrm{BF}}}{m}\delta n_f(\mathbf{r})\right], \quad (5)$$

where we have identified the dimer-fermion scattering length a_{BF} which takes the Born value $8a_{\mathrm{F}}/3$ at the mean-field level. We obtain, in addition,

$$c_0(\mathbf{r}) = -\frac{\partial}{\partial\mu_\uparrow}\frac{\partial}{\partial\mu_\downarrow}a_0(\mathbf{r}) \cong -\frac{m^3 a_{\mathrm{F}}^3}{16\pi} + m^2 a_{\mathrm{F}}^4\frac{\partial\delta n_f(\mathbf{r})}{\partial\mu_\uparrow}. \quad (6)$$

The gap equation (2) eventually reduces to the following equation for the condensate wave function $\Phi(\mathbf{r}) = \sqrt{m^2 a_{\mathrm{F}}/(8\pi)}\Delta(\mathbf{r})$:

$$-\frac{\nabla^2}{2m_{\mathrm{B}}}\Phi(\mathbf{r}) + \left[2V(\mathbf{r}) + \frac{3\pi a_{\mathrm{BF}}}{m}\delta n(\mathbf{r})\right]\Phi(\mathbf{r}) + \frac{4\pi a_{\mathrm{B}}}{m_{\mathrm{B}}}|\Phi(\mathbf{r})|^2\Phi(\mathbf{r}) = \mu_{\mathrm{B}}\Phi(\mathbf{r}), \quad (7)$$

where $m_{\mathrm{B}} = 2m$ is the dimer mass and the dimer-dimer scattering length a_{B} takes the Born value $2a_{\mathrm{F}}$ at the mean-field level. Note how the last term in Eq. (6) combines with the term proportional to δn_f in Eq. (5), to yield in Eq. (7) the *density of excess fermions*:

$$\begin{aligned} \delta n(\mathbf{r}) &= \delta n_f(\mathbf{r}) - \frac{3\pi a_{\mathrm{BF}}}{m}|\Phi(\mathbf{r})|^2\frac{\partial\delta n_f(\mathbf{r})}{\partial\mu_\uparrow} \\ &\cong \int\frac{d\mathbf{k}}{(2\pi)^3} f\left[\frac{\mathbf{k}^2}{2m} + V(\mathbf{r}) + \frac{3\pi a_{\mathrm{BF}}}{m}|\Phi(\mathbf{r})|^2 - \mu_\uparrow\right]. \end{aligned} \quad (8)$$

By this mechanism, Eq. (7) contains the effect of the fermionic distribution $\delta n(\mathbf{r})$ on the bosonic one, an effect which is reciprocated in Eq. (8) by the bosonic distribution $|\Phi(\mathbf{r})|^2$ on the fermionic one.

The final equation results from considering the total density $n(\mathbf{r}) = n_\uparrow(\mathbf{r}) + n_\downarrow(\mathbf{r})$ where:

$$\begin{aligned} n(\mathbf{r}) &= \frac{1}{\beta}\sum_s[e^{i\omega_s\eta}G_{11}(\mathbf{r},\mathbf{r};\omega_s) - e^{-i\omega_s\eta}G_{22}(\mathbf{r},\mathbf{r};\omega_s)] \\ &\cong \delta n(\mathbf{r}) + 2|\Phi(\mathbf{r})|^2. \end{aligned} \quad (9)$$

Equations (7) and (9), together with the definition (8), are the desired closed set of equations which determine $\Phi(\mathbf{r})$ and $\delta n(\mathbf{r})$ in the BEC limit, for given total number of fermions $N_\uparrow + N_\downarrow = \int d\mathbf{r}n(\mathbf{r})$ and density imbalance $N_\uparrow - N_\downarrow = \int d\mathbf{r}\delta n(\mathbf{r})$.

The validity of these equations can be extended by improving on the values of the scattering lengths a_{BF} and a_{B}. At the mean-field level so far considered, these values correspond to the Born approximation, yielding $a_{\mathrm{BF}} = 8a_{\mathrm{F}}/3$ and $a_{\mathrm{B}} = 2a_{\mathrm{F}}$. The exact value $1.18a_{\mathrm{F}}$ of a_{BF} has been known for some time [8], while the exact value $0.6a_{\mathrm{F}}$

of $a_{\rm B}$ was determined only recently [9]. These values have also been obtained by diagrammatic methods in the limit of vanishing density, for $a_{\rm BF}$ in Ref. [10] and for $a_{\rm B}$ in Ref. [11]. To improve on the derivation of Eqs. (7) and (9), so as to include the exact values of $a_{\rm BF}$ and $a_{\rm B}$, we thus need to identify additional fermionic diagrams beyond mean field, which contain the correct diagrammatic sequences for $a_{\rm BF}$ and $a_{\rm B}$ as subunits. This can be achieved as follows.

In the BEC limit, the gap equation can be interpreted as the condition of vanishing "tadpole" insertions for composite bosons, with a natural extension of what is done for pointlike bosons [12]. Within mean field, the diagrams representing this condition are depicted in Fig. 1(a). Here, a composite-boson propagator with zero four-momentum can be inserted from the left, while the gap Δ corresponds to a condensate line. We have already shown that these diagrams contain the dimer-fermion and dimer-dimer scattering processes within the Born approximation. Additional tadpole diagrams, whose effect is to modify the values of $a_{\rm BF}$ and $a_{\rm B}$ in Eq. (7), are depicted in Figs. 1(b) and 1(c) in the order. These diagrams exclude the Born contributions already included in the mean-field diagrams of Fig. 1(a). A comment is in order on how to factor out from the diagrams of Fig. 1(b) the product $a_{\rm BF}$ times δn that enters Eq. (7). From the structure of these diagrams one concludes that the integration over the wave vector $\mathbf{P}$ is bounded within the Fermi sphere with radius $\sqrt{2m\mu_\uparrow}$, while the remaining integrations over the wave vectors $\mathbf{q}$, $\mathbf{q}', \ldots$ extend outside this Fermi sphere. Accordingly, one may neglect the P dependence everywhere in the diagrams of Fig. 1(b), *except* in the fermion propagator labeled by P and corresponding to a spin-$\uparrow$ fermion. The density of excess fermions results in this way from the P integration, while the remaining parts of the diagrams yield the exact dimer-fermion scattering matrix $T_3'(0)$, which excludes the Born contribution resulting from mean field.

A similar analysis can be carried out for the density Eq. (9), where only the value of the dimer-fermion scattering length $a_{\rm BF}$ needs to be corrected beyond mean field [cf. Eq. (8)].

We thus solve the coupled Eqs. (7) and (9) with the exact values of $a_{\rm BF}$ and $a_{\rm B}$. To make contact with the recent experimental findings [1,2], we determine the density profiles $\delta n(\mathbf{r})$ and $n_0(\mathbf{r}) = |\Phi(\mathbf{r})|^2$ by solving these equations in the Thomas-Fermi approximation for a spherical trap, as functions of the *asymmetry parameter* $\alpha = (N_\uparrow - N_\downarrow)/(N_\uparrow + N_\downarrow)$ (with $0 \le \alpha \le 1$).

In Fig. 2 we report the density profiles $\delta n(r)$ and $n_0(r)$ versus the distance $r = |\mathbf{r}|$ from the center of the trap, for

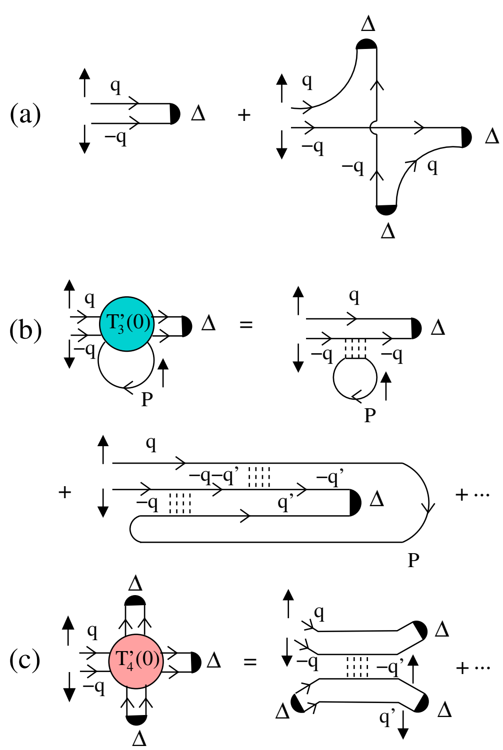

FIG. 1 (color online). Tadpole diagrams for composite bosons representing the gap equation in the BEC limit: mean-field contributions (a), contributions including the dimer-fermion (b), and dimer-dimer (c) scattering processed beyond the Born approximation. Full line: fermionic propagator of given spin; broken line: fermionic interaction v_0.

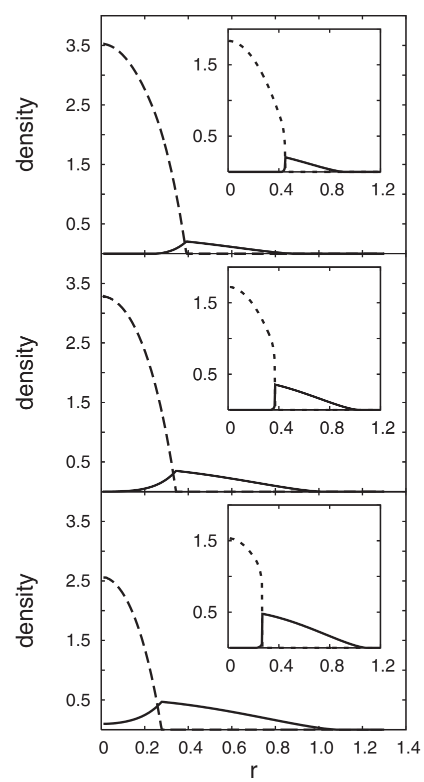

FIG. 2. Density profiles $\delta n(r)$ (full lines) and $n_0(r)$ (broken lines) vs $r = |\mathbf{r}|$ for $(k_{\rm F}a_{\rm F})^{-1} = 3$ and $\alpha = 0.2$ (upper panel), $\alpha = 0.5$ (middle panel), $\alpha = 0.8$ (lower panel) [r is in units of $R_{\rm TF}$ and densities are in units of $(N_\uparrow + N_\downarrow)/R_{\rm TF}^3$]. The insets show the results for $(k_{\rm F}a_{\rm F})^{-1} = 1$ at the same values of α. Here, $R_{\rm TF}$ and $k_{\rm F}$ are the Thomas-Fermi radius and Fermi wave vector for equal populations.

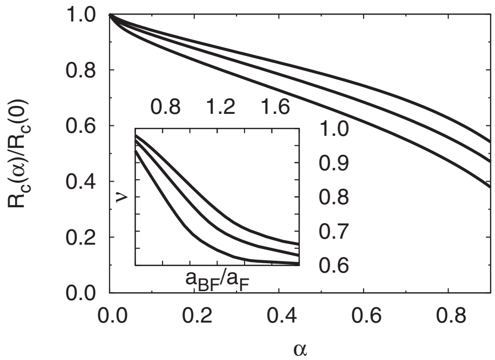

FIG. 3. Critical radius R_c of the condensate density vs the asymmetry parameter α [normalized to the value $R_c(0)$ at $\alpha = 0$] for the coupling values $(k_F a_F)^{-1} = (1, 2, 3)$ from bottom to top. The inset shows the ratio ν between the column density of excess fermions at the center of the trap and its maximum value at R_c vs a_{BF}/a_F, for $\alpha = 0.5$ and the coupling values $(k_F a_F)^{-1} = (2, 3, 4)$ from bottom to top.

three characteristic values of α and for the coupling $(k_F a_F)^{-1} = 3$ on the BEC side of the crossover. The spatial separation between the condensed composite bosons and the excess fermions is evident from these plots [13]. For the coupling here considered, this phase separation occurs for all values of α, because $\delta n(r)$ tends to set outside the region occupied by $n_0(r)$. Note that, for each value of α, the maximum of $\delta n(r)$ occurs where $n_0(r)$ vanishes. Note also the progressive shrinking of $n_0(r)$ for increasing α, with a simultaneous penetration of $\delta n(r)$ toward the center of the trap. The presence of both n_0 and δn in the same spatial region can be related to the occurrence of the homogeneous gapless superfluid which was discussed in Ref. [6]. The insets show the results for the smaller coupling $(k_F a_F)^{-1} = 1$. The phase separation between the two species appears sharper in this case, corresponding to enhanced effects of the dimer-fermion repulsion. [By solving also the full differential equation (7) we have verified that this sharp phase separation remains, apart from a minor rounding of the edges, for the typical particle numbers considered in the experiments.]

We have verified that for the column density profiles considered in the experiments (which result from the above profiles by integrating over, say, the z axis) the phase separation appears less evident even for $(k_F a_F)^{-1} = 1$, since the corresponding distribution $\int dz \delta n(\rho, z)$ leaks toward $\rho = 0$ where it acquires a finite value.

Our calculation does not reveal evidence for a critical value α_c below which phase separation does not occur. This contrasts with the experimental claim of Ref. [2], where at unitarity α_c was estimated to be about 0.10. [14].

In Fig. 3 the critical radius R_c of the condensate density is plotted versus α for different couplings, showing specifically how the condensate density shrinks for varying α and coupling. This quantity should have direct experimental access, because it identifies also the position of the maximum of the density of excess fermions. This maximum value can be compared with the value of the excess density at the center of the trap, to determine how their ratio ν depends on the dimer-fermion scattering length a_{BF} (assuming that the value of a_B is independently determined). Column density profiles are found to have a more marked dependence on a_{BF} than density profiles. Accordingly, in the inset of Fig. 3 we report the corresponding ratio ν versus a_{BF} for $\alpha = 0.5$ and different couplings. The rather marked dependence on a_{BF} shown by this quantity should make it possible to extract from the experimental data the expected value 1.18 of a_{BF}/a_F, using our plots for calibration.

[1] M. W. Zwierlein, A. Schirotzek, C. H. Schunck, and W. Ketterle, Science **311**, 492 (2006).
[2] G. B. Partridge *et al.*, Science **311**, 503 (2006).
[3] R. Combescot, Europhys. Lett. **55**, 150 (2001); W. V. Liu and F. Wilczek, Phys. Rev. Lett. **90**, 047002 (2003); H. Caldas, Phys. Rev. A **69**, 063602 (2004); A. Sedrakian, J. Mur-Petit, A. Polls, and H. Müther, Phys. Rev. A **72**, 013613 (2005).
[4] T. Mizushima, K. Machida, and M. Ichioka, Phys. Rev. Lett. **94**, 060404 (2005); P. Castorina *et al.*, Phys. Rev. A **72**, 025601 (2005).
[5] U. Lombardo *et al.*, Phys. Rev. C **64**, 064314 (2001); T. D. Cohen, Phys. Rev. Lett. **95**, 120403 (2005); C. Pao, S. Wu, and S. Yip, cond-mat/0506437; D. T. Son and M. A. Stephanov, cond-mat/0507586; D. E. Sheehy and L. Radzihovsky, Phys. Rev. Lett. **96**, 060401 (2006).
[6] J. Carlson and S. Reddy, Phys. Rev. Lett. **95**, 060401 (2005).
[7] P. Pieri and G. C. Strinati, Phys. Rev. Lett. **91**, 030401 (2003).
[8] G. V. Skorniakov and K. A. Ter-Martirosian, Sov. Phys. JETP **4**, 648 (1957).
[9] D. S. Petrov, C. Salomon, and G. V. Shlyapnikov, Phys. Rev. Lett. **93**, 090404 (2004).
[10] P. F. Bedaque and U. van Kolck, Phys. Lett. B **428**, 221 (1998).
[11] I. V. Brodsky *et al.*, JETP Lett. **82**, 273 (2005).
[12] V. N. Popov, *Functional Integrals and Collective Excitations* (Cambridge University Press, Cambridge, England, 1987).
[13] A similar phase separation is found when considering mixtures of bosonic and fermionic atoms for certain values of the phenomenological parameters [see R. Roth, Phys. Rev. A **66**, 013614 (2002)].
[14] These experimental data are currently subject of controversy (see M. W. Zwierlein and W. Ketterle, cond-mat/0603489).